PCCP

PAPER

View Article Online
View Journal | View Issue

Cite this: *Phys. Chem. Chem. Phys.*, 2025, **27**, 24994

Ionene-based physical hydrogels: probing the liquid-gel transition, chain and counterion dynamics by means of NMR

Sarrah Mezdari,[a] Lingsam Tea,[a] Juliette Sirieix-Plénet,[a] François Ribot[b] and Natalie Malikova *[a]

Ionene-based physical hydrogels have been investigated here in terms of the changes of the local environment for ionene polyelectrolyte chains and their counterions upon the liquid-gel transition. These changes were probed *via* ^{1}H and ^{19}F NMR chemical shifts, peak intensities and peak broadening. Further, chain and counterion dynamics was studied by means of PFG-NMR. Properties of ionene-based hydrogels being highly sensitive to the nature of the chain counterion, we compare here two systems, with F^- and Cl^- counterions. An important observation is the significant loss of signal intensity for the ionene chains and counterions upon the liquid-gel transition. This is a consequence of the immobilisation of a proportion of the chains and counterions as they start taking part in the cross-linked chain network and become invisible to solution/liquid state NMR. For the counterions (measured only in the case of ^{19}F nuclei), the liquid-gel transition leads also to a sudden deshielding effect (peak shift by 3 ppm) and a large increase in the peak width (decrease in the ^{19}F transverse relaxation time). This clearly attests to the involvement of the counterions in the formation of chain cross-links in ionene-based hydrogels. For all solution/liquid and gel phases, the diffusion coefficients of NMR-visible chains are consistently higher in the case of Cl-gels, in comparison to F-gels (a factor of $\approx$ 2). This reflects the increased rigidity of the F-ionene chains due to strong dissociation of the strongly hydrating F^- ions from the ionene backbone.

Received 9th July 2025,
Accepted 31st October 2025

DOI: 10.1039/d5cp02615f

rsc.li/pccp

1 Introduction

Hydrogels, as the most typical elastomer materials with three-dimensional (3D) network structures, based on biopolymers or synthetic polymers (both neutral or charged) in water, have attracted much attention due to applications in numerous fields, including food, pharmaceuticals, agriculture, chemical processing, and electronics.[1] Regarding physical hydrogels, their main feature is a reversible transition between the gel and solution (or liquid) states, as the gelation is based on non-covalent chain–chain interactions such as hydrogen bonding, π–π stacking, van der Waals, charge transfer and electrostatic interactions. Charged polymers, or polyelectrolytes (PEs), are of fundamental and practical importance since many of them play critical biological functions as well as being used in many industrial fields, including food, packaging, paints and surface treatments *etc.*[2–4] Within PEs, synthetic ionenes represent an important subgroup in which the ionic groups form part of the polymer backbone.[5–8] The term ionenes is further restricted to positively charged PEs carrying a quaternary nitrogen group as the charged center.[9] Ionenes can form stable hydrogels thanks to their considerable structural versatility, by introducing gel-forming moieties, based on aromatic rings, into the ionene structure (see Fig. 1).[10–14]

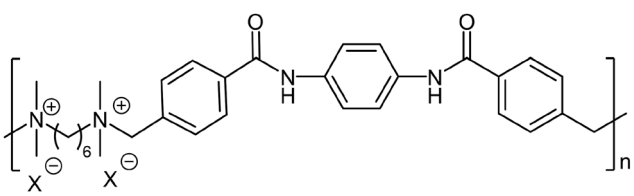

Fig. 1 Structure of poly[(dimethylimino) hexane-1,6 diyl(dimethylimino)-methylene-1,4-phenylenecarbonylimino-1,4-phenylene-iminocarbonyl-1,4-phenylenemethylene dihalide], X = Cl^- or F^- as counterions. Ionene solutions/gels based on this structure are denoted from now on as 6-Cl or 6-F ionenes, where 6 represents the number of methylene groups (CH_2) between the two charged quaternary ammonium centres inside the aliphatic chain of each monomer.

[a] *Sorbonne Université, CNRS, Laboratory of Physical Chemistry of Electrolytes and Interfacial Nanosystems (PHENIX), 4 place Jussieu, F-75005 Paris, France. E-mail: natalie.malikova@sorbonne-universite.fr*

[b] *Sorbonne Université, CNRS, Laboratoire de la Chimie de la Matière Condensée de Paris (LCMCP), 4 place Jussieu, F-75005 Paris, France*

In the context of this manuscript, hydrogels are considered as a highly flexible and permeable matrix for the diffusion of potential guest species,[15] as is of highest pertinence for applications of hydrogels in drug delivery, tissue engineering or, to start with, as models of extracellular matrix.[16] In recent publications we have shown that the structure and rheological properties of ionene gels is highly sensitive to the nature of the ionene counterion (mainly halide counterions have been studied). Not only does the counterion influence the critical gelation concentration (CGC), but also the elastic modulus (G') of the gel.[13] The typical mesh-size of ionene gels is 20 nm, but additional smaller mesh sizes were observed for ionene hydrogels with fluoride counterions. For conventional ionenes (no gel-forming moieties present in the structure), it has been repeatedly observed that chain–chain electrostatic interactions and the chain rigidity are influenced by the nature of the counterion, due to different degrees of "ion-specific screening".[17–19] The goal of this manuscript is to investigate, by means of NMR, firstly the changes taking place in the local environment of the chains and counterions (NMR chemical shifts), as we pass from the solution/liquid to the gel phase and, secondly, the mobility of the ionene chains and the counterions in ionene hydrogels (by pulsed field gradient NMR), reflecting to some extent the flexibility of the hydrogel matrix itself. This is an interesting step prior to investigating the mobility of any guest species in these hydrogels. Diffusion of molecules/colloids in flexible or fluctuating matrices is indeed influenced by the coupling between the guest and host dynamics.[20]

In broad terms, on the local, molecular scale, NMR gives insight into the variation of the spin environment, *via* changes in the chemical shift.[21] This can be employed to study the conformation and structure of polymer chains[22] or evaluate the association of ions and charged chains.[23–25] On a larger length scale (10–100 μm), pulsed field gradient NMR (PFG-NMR) has proven to be a valuable technique that probes the mobility of ions or charged/uncharged polymer chains[26,27] and has been successfully applied to gels.[10,28–31]

2 Experimental section

2.1 Hydrogel preparation

All chemical reagents and solvents were purchased from Sigma-Aldrich and VWR and used without further purification. Ionene PEs were synthesized *via* a two-step reaction with a protocol adapted from the one described previously[10,12,13] to obtain PE chains with a structure as depicted in Fig. 1. In brief, step (a) of the two-step reaction corresponds to the amidation reaction of 4-(chloromethyl)benzoyl chloride and *p*-phenylenediamine (in the presence of triethylamine) in CH_2Cl_2. It yields 1,4-bis[4-(chloromethyl)benzamido] benzene (refer to its ^{1}H NMR spectrum in Fig. S1 of SI). This is the aromatic part of the future ionene monomer and has electrophilic benzyl parts at its termini. In step (b) it is used as a dielectrophilic monomer for the polymerization (poly-addition) reaction: equimolar mixtures of 1,4-bis[4-(chloromethyl)benzamido benzene and *N*,*N*,*N*′,*N*′-tetramethyl-1,6-hexanediamine, as the dinucleophilic monomer, were stirred at 80 °C for 48 h in DMF to give the corresponding 6-Cl ionene PEs, as precipitates in high yields (83–94% after purification). According to literature, the molecular weights of the resulting gel-forming ionenes are rather small, less than 100 kDa (78 kDa indicated in ref. 10). The default counterion of gel-forming ionene PEs is the Cl^- ion, other ions such as F^- can be obtained by exchange dialysis. A solution of 6-Cl at a concentration of 0.01 mol L^{-1}, lower than the critical gelation concentration CGC (9.5 g L^{-1}, 0.016 mol L^{-1}), was prepared by heating at 70 °C for 10 minutes to ensure complete solubilisation and then cooling back to room temperature. The solution was then introduced into the dialysis cassette Slide-A-Lyzer with a cut-off of 10 kDa. The dialysis was carried out 3 times against 0.05 mol L^{-1} NaF solution for 24 h each. The excess salt was removed by 5 successive baths of ultra pure water. We checked that all the excess salt was removed by measuring the conductivity of the bath (the conductivity was equal to the one of ultra pure water after 5 successive baths). The contents of the dialysis cassette was then collected and freeze-dried to remove water. Solutions and gels at a given concentration were thereafter prepared by measuring out the appropriate mass of the freeze-dried samples. Thermogravimetric analysis on the powder samples was performed to account for residual water and thus correct the final solution/gel concentrations.

In the rest of manuscript we refer to the gel-forming ionenes with Cl^- and F^- counterions as 6-Cl and 6-F respectively. We already reported that the solubility in water as well as the critical gelation concentration (CGC) of gel-forming ionene PEs is strongly dependent on the nature of the counterion.[13] While 6-F ionenes are soluble in water at room temperature, 6-Cl ionenes are only partially soluble at room temperature. In order to prepare ionene hydrogels, ionene PEs were dissolved/dispersed in deionized water or D_2O and heated up to 80 °C to maximize the solubilization. For concentrations above CGC, the gelation occurs upon cooling down to room temperature. The gelation ability of the ionene polymers was tested by the vial inversion method.

2.2 NMR and PFG-NMR measurements

All samples for NMR measurements were prepared in D_2O (Merck, 99.8%). The solutions were heated to 80 °C and transferred to 5 mm NMR tube for analysis. The gels formed directly inside the NMR tubes by cooling down to room temperature. For both ^{1}H and ^{19}F nuclei, chemical shifts, peak intensity and self-diffusion coefficients (by PFG-NMR) were measured. All NMR measurements were carried out at 18 °C. At least 10 minutes were allowed for temperature equilibration before collecting NMR data. Topspin 4.0.4 software was used for processing all spectra.

PFG-NMR measurements were performed on a Bruker AvanceIII 300 MHz (7.05 T) spectrometer, using a 5 mm BBFO probe equipped with z-gradient coil providing a maximum gradient strength of 50.8 Gauss cm^{-1}. We used a stimulated echo sequence (ledbpgp2s) with longitudinal eddy current delay (T_e = 5 ms) and bipolar smoothed-square shaped gradient

pulses for the measurements of diffusion coefficients. 16 gradient increments, linearly spaced from 2% to 90% of the maximum gradient strength, were used. Self-diffusion coefficients D for selected ions (F^-), water and ionene PE chains were determined by fitting the integral of the echo obtained for variable gradient strengths, using the Stejskal–Tanner equation[32]

$$I = I(g=0)\exp\left[(\gamma g\delta)^2 D\left(\Delta - \frac{\delta}{3}\right)\right] \quad (1)$$

where I is the observed integral for a given gradient strength g (which includes the correction for the gradient shape), $I_{(g=0)}$ is the integral when the gradient strength equals zero, D is the self-diffusion coefficient, γ is the gyromagnetic ratio of the observed nucleus (^{1}H or ^{19}F), δ is the length of the gradient pulse (twice the length of the bipolar pulses) and Δ is the diffusion time. Experiments were conducted with diffusion time Δ ranging from 200 to 250 ms and the gradient pulse duration δ was from 0.8 to 4 ms. For each measurement, Δ and δ were chosen to achieve an attenuation greater than 90% for the last gradient strength.

3 Results and discussion

3.1. ^{1}H NMR: interactions and mobility of ionene chains in liquid and gel phases

^{1}H spectrum of a 8 g L^{-1} (0.014 mol L^{-1}) solution of 6-F modified ionene in D_2O is shown in Fig. 2. The ^{1}H spectrum is consistent with previously reported results.[10,13] For completeness, the ^{1}H NMR spectrum of 6-Cl modified ionene in DMSO-d6/D_2O at 1/1 (v/v) is shown in the SI (Fig. S2), showing sharper peaks in this higher quality solvent. For the remainder of this manuscript, we are however interested in aqueous solutions and gels of ionenes. For further purposes we distinguish two families of proton peaks in Fig. 2: (a) aromatic protons (H_a to H_c) and (b) aliphatic protons (d to h), which are depicted in the schematic drawing of the ionene structure in Fig. 2 (bottom).

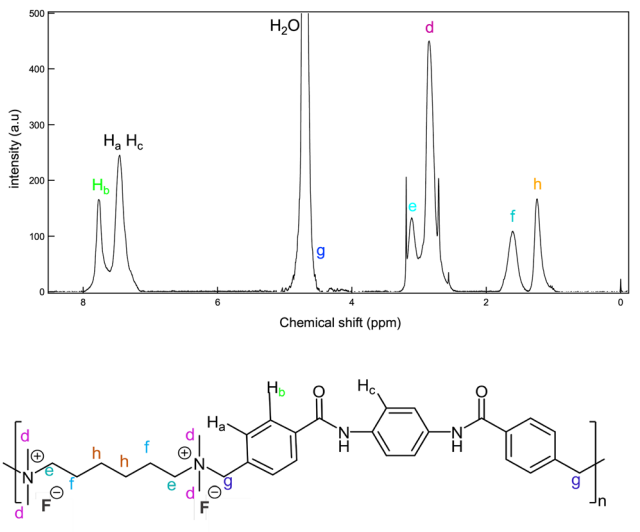

Fig. 2 Top: ^{1}H NMR of 6-F ionene solution at 8 g L^{-1} (0.014 mol L^{-1}, 300 MHz, D_2O solvent). Aromatic protons (H_a, H_c and H_b) appear at chemical shifts around 7–8 ppm, while aliphatic protons (d to h) appear in the range of 1.2–4.6 ppm. The strongest peak at 2.8 ppm (d) corresponds to methyl groups directly attached to the charged quaternary ammonium centers. Bottom: A schematic drawing of the ionene structure, indicating the different chemical environments for aromatic and aliphatic protons.

In the comparison of ^{1}H spectra of ionene solutions *versus* ionene gels, we were particularly interested in the signal of the aromatic protons. As reported in the literature, ionene gel formation is based on the attractive chain–chain interaction between the benzene moieties of the ionene monomer, particularly *via* π–π stacking.[10,11] We therefore investigated whether the signature of π–π stacking in the gel phase could be observed *via* the chemical shifts of the aromatic protons. Fig. 3 features the position of the peak corresponding to the H_b family, which in the solution phase is placed at 7.8 ppm. However, no visible difference is observed in these aromatic proton shifts on transition from the solution/liquid to the gel state, be it for the 6-F or the 6-Cl system.

The lack of change in the chemical shift of aromatic protons is at first sight surprising, though the literature reports upon other systems, where shifts in aromatic protons are minimal, while shifts in amide protons (due to hydrogen bond formation) are much more significant.[33] The next question is whether we retain visibility of all the chains (and thus H_b family protons) once the gel phase is formed. Fig. 4 features the integrals of the proton peaks corresponding to the H_b family, as a function of the ionene concentration, spanning both the solution/liquid and gel phase. Let us concentrate at first on the 6-F data. In the solution phase, we see a clear linear dependence of the integral with increasing ionene concentration and at CGC a sudden drop to significantly lower values. If we extrapolate the initial linear dependence into the gel phase, we can estimate the expected integrals if all chains (and thus H_b family protons) were visible in the entire concentration range. Once the gel is formed, we loose the NMR signal

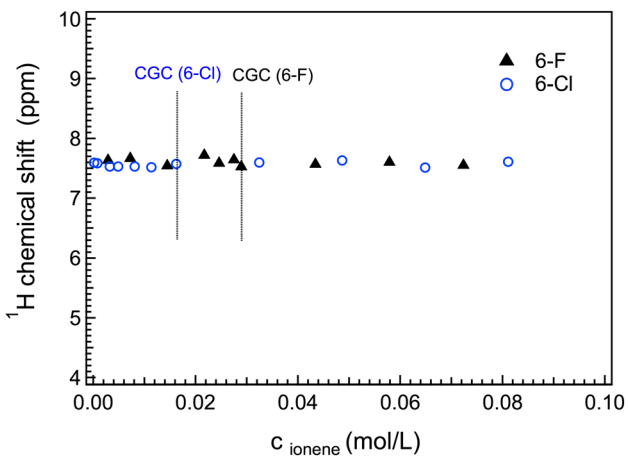

Fig. 3 ^{1}H chemical shifts for aromatic protons (H_b family), as a function of ionene concentration. The vertical lines indicate the critical gel concentration for each system, 0.017 mol L^{-1} for 6-Cl and 0.036 mol L^{-1} for 6-F. The error bar is at most the size of the symbols.

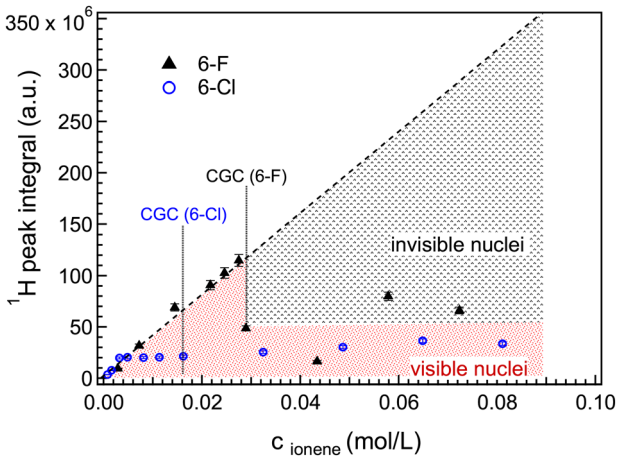

Fig. 4 Integrated intensities of NMR peak of the H_b family, as a function of 6-F or 6-Cl ionene concentration in D_2O. The grey and red regions represent respectively the invisible and visible nuclei (*i.e.* chains) for the 6-F system.

from a significant proportion of the chains (from roughly 50% at the CGC to over 80% at the highest 6-F ionene concentration – see the grey shaded region in Fig. 4). In addition, we traced the ^{1}H integrated signal as a function of time, over several tens of hours (see Fig. S3 in the SI). Indeed, as gelation proceeds, a signal loss is observed, with the most significant drop taking place in the first 10 hours. Overall, Fig. 4 informs us that upon gelation, a significant proportion of the ionene chains is lost to solution NMR. These "immobilised" chains are forming the cross-linked chain network, which is the basis of the gel structure. The broadening and disappearance of signals corresponding to polymer chains (^{1}H NMR) on the solution/liquid to gel transition has been observed several times in the past.[33–35] We show further in this manuscript that for polyelectrolyte based hydrogels, an analogous immobilisation of the chain counterions equally takes place for ionene-based hydrogels, as they become involved in the formation of the chain cross-links.

The situation is somewhat different for the 6-Cl data in Fig. 4, for which even in the solution phase the expected linear dependence is not seen. We observe lower integrals than expected already prior to CGC (taking the 6-F data as a reference). This is linked to the poorer solubility of the 6-Cl system in the water solvent. It is well known for ionene polyelectrolytes, that fluoride counterions render the system most soluble in water, in comparison to other halide ions.[18] The low peak integrals for the 6-Cl data series have thus two origins, insufficient solubility of the 6-Cl system, on top of which is added the effect of gelation beyond the corresponding CGC (0.016 mol L^{-1}).

Remaining with the signal of the aromatic protons (H_b and H_a, H_c), we used PFG-NMR to measure the corresponding self-diffusion coefficient, taking it as a measure of the self-diffusion of the visible ionene chains, in the solution and gel phases. In all cases the PFG-NMR decays were fitted with a mono-exponential decay. Overall, this leads to an estimate of an average diffusion coefficient of all visible chains in the sample. Examples of the PFG-NMR decays are given in the SI (Fig. S4). We note that while for some systems a mono-exponential fit was satisfactory, for others a visible departure from mono-exponential decay was observed. However, no clear trends as a function of ionene concentration were detected. Any observed departure from mono-exponential behaviour can be attributed to several factors, including the heterogeneity of the hydrogel network and thus a multi-mode diffusion (restricted diffusion within certain regions of the hydrogel) or indeed chain length polydispersity. Chain length polydispersity is indeed a known issue for ionene based polyelectrolyte chains, and their polydispersity index can be very high, reaching values of 2.[19] Similarly, sample heterogeneity is very likely, as shown by our previous small angle X-ray scattering (SAXS) data, where two different mesh sizes of the gel were revealed for the 6-F system, as well as large scale heterogeneities for both 6-F and 6-Cl.[13] More generally, in the study of complex polymer systems it is common to observe a departure from a mono-exponential decay of the spin echo signal.[36,37] A number of investigations[36,38–40] on associating polymer systems show that the spin-echo attenuation data can be well described by a stretched exponential, reflecting an entire distribution of diffusion coefficients. When departure from a mono-exponential decay was clearly observed in our samples, we performed measurements with different diffusion times and checked that the observation of two diffusion coefficients were not related to an intermediate exchange on the diffusion time scale (see Fig. S5 of SI).

Fig. 5 summarizes the self-diffusion coefficients of the visible chains for 6-F and 6-Cl systems. Let us concentrate first on the 6-F data set. Remember that in the 6-F solution, all the chains are visible, while only some chains remain visible in the 6-F gel phase (refer back to Fig. 4). Fig. 5 shows no significant drop in the diffusion coefficient at the CGC of 6-F, thus the non-crosslinked, free (visible) chains in the gel phase diffuse with the same diffusion coefficient as the free chains at

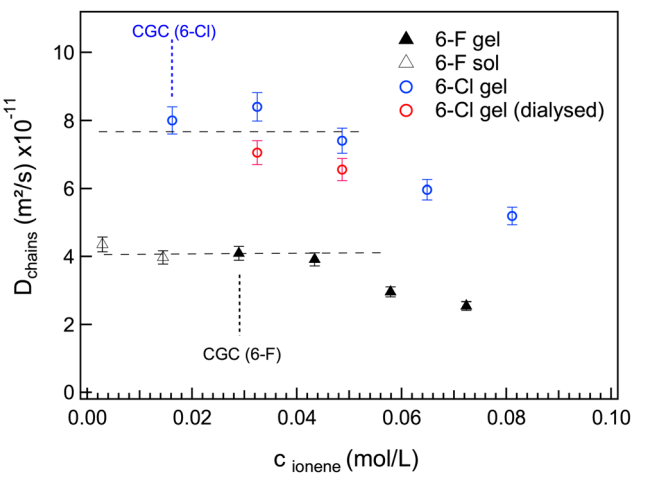

Fig. 5 Self-diffusion coefficients of visible ionene chains as a function of ionene concentration for 6-Cl and 6-F systems, in the solution and gel phases. CGC for each system is represented by a vertical dashed line. Horizontal dashed lines are guides to the eye. Measurements done at 18 °C.

concentrations below the CGC. For the two highest 6-F gel concentrations the diffusion of the free chains is hindered and slowed down by approximately a factor of 2. A similar trend is seen for 6-Cl (no solution data is available), only the two highest gel concentrations show a marked decrease in the diffusion coefficient of the non-crosslinked, free (visible) chains. Importantly, the entire data set for 6-Cl is above that of 6-F. In other words, irrespective of the concentration, the free chains diffuse faster (by a factor of cca 2) in the 6-Cl gels than in the 6-F gels. A side note is in place: since the 6-F system was obtained *via* dialysis of the 6-Cl against NaF, we first considered that the dialysis shifted the size distribution of the ionene chains towards longer chains for the 6-F (short ionene chains lost in ion exchange dialysis). However, we were able to discard this scenario as even after dialysing 6-Cl samples, the non-crosslinked chain diffusion in 6-Cl gels is still faster than in 6-F gels, see data set "6-Cl (dialysed)".

We propose here two possible explanations for the faster self-diffusion of the non-crosslinked chains in 6-Cl gels in comparison to 6-F gels. The first is related to previous scattering studies and simulations on conventional ionenes (containing no aromatic moieties in the ionene structure), which have shown a more dissociated form of counterions in the case of F^-, as opposed to all other halide ions, due to their different hydration energies.[17–19,41] In contrast to all heavier halide ions, F^- has the most negative hydration energy, the ion retains its hydration shell in the vicinity of the ionene, behaves as a fully solvated dissociated ion, thus maintaining a full charge on the ionene backbone. For the heavier, more weakly hydrated halide ions such as Cl^- or Br^-, water molecules are stripped away on approach to the ionene chain, a closer contact is possible, the chain charge is screened more effectively and the chains are more flexible. This renders F-ionenes (conventional and gel-forming) indeed more water-soluble than any of their Cl^- or Br^- analogues. The more significant counterion dissociation in the case of F^- renders the chains more charged and thus more rigid, which would lead to a decrease in their self-diffusion coefficient observed by PFG-NMR. This was indeed already observed in solutions of conventional ionenes.[19] The second explanation is linked to the presence of a tighter mesh size measured by SAXS for the 6-F gels, an effect accentuated at high 6-F gel concentration.[13] A denser network of cross-links would indeed also lead to a decreased chain self-diffusion coefficient of the free non-crosslinked chains.

3.2. ^{19}F NMR: interaction and mobility of chain counterions in liquid and gel phases

Having highlighted the importance of counterion nature in solutions and gels of ionenes, in this section we analyse the local environment and self-diffusion of the fluoride counterions in 6-F systems, ^{19}F nuclei being highly abundant dipolar nuclei, with easy NMR detection. As depicted in Fig. 6, the ^{19}F NMR spectra of 6-F ionenes show a marked change upon gelation. Note that all samples, below and above the CGC, were subjected to an identical heat treatment (refer back to the experimental section). In the solution state (0.003 to

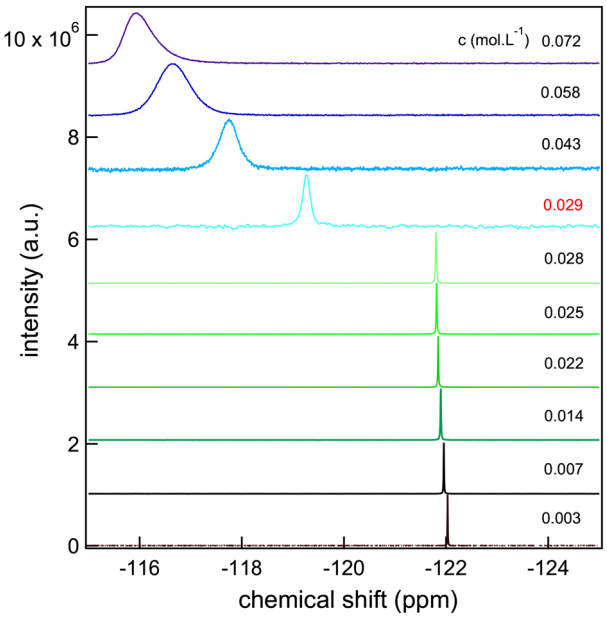

Fig. 6 Series of full ^{19}F NMR spectra for 6-F ionene systems spanning the solution/liquid and the gel state. CGC is indicated in red. The spectra were shifted and rescaled in *y* axis for clarity.

0.028 mol L^{-1}) a single sharp singlet is seen, appearing at −122.0 ppm for the lowest concentration and shifting slightly downfield as the ionene concentration increases (by 0.2 ppm for 0.028 mol L^{-1}). Upon gelation (CGC marked in red in Fig. 6), the spectrum shows a sudden downfield shift of 3 ppm and a significant peak broadening. As the gel concentration increases, further downfield shift is seen, as well as increased peak broadening.

Fig. 7 summarizes quantitatively several important features of the ^{19}F spectra from Fig. 6, namely (a) the integral of the fluoride peak, assessing the total/partial visibility of the entire fluoride ion population, akin to Fig. 4 for the ionene chains, (b) the chemical shift, compared to an NaF reference and (c) the broadening of the peak, expressed as the T_2^* relaxation time. The NaF reference featured in Fig. 7 (top and center) corresponds to NaF aqueous solutions at concentrations that match the counterion concentrations in the corresponding ionene solutions/gels. The ionene counterion concentration is obtained by multiplying the ionene monomer concentration by two, since there are two F^- ions per monomer (refer back to Fig. 1).

Fig. 7 (top) demonstrates clearly a decrease in the integrated intensity for the ^{19}F NMR peak for the two highest gel concentrations. The proportion of the invisible counterions above CGC is lower than in the case of the chains (refer back to Fig. 4), reaching only about 20% at the highest 6-F concentration. As for the chains, a subfamily of the fluoride counterions becomes immobilised within the gel and is no longer detectable by solution NMR, though this happens not immediately at the CGC, but for higher gel concentrations. It is interesting to comment on the data of the NaF reference series. The NaF data and the 6-F solution data fall indeed onto the same linear "master" curve, which confirms unquestionably that all ^{19}F

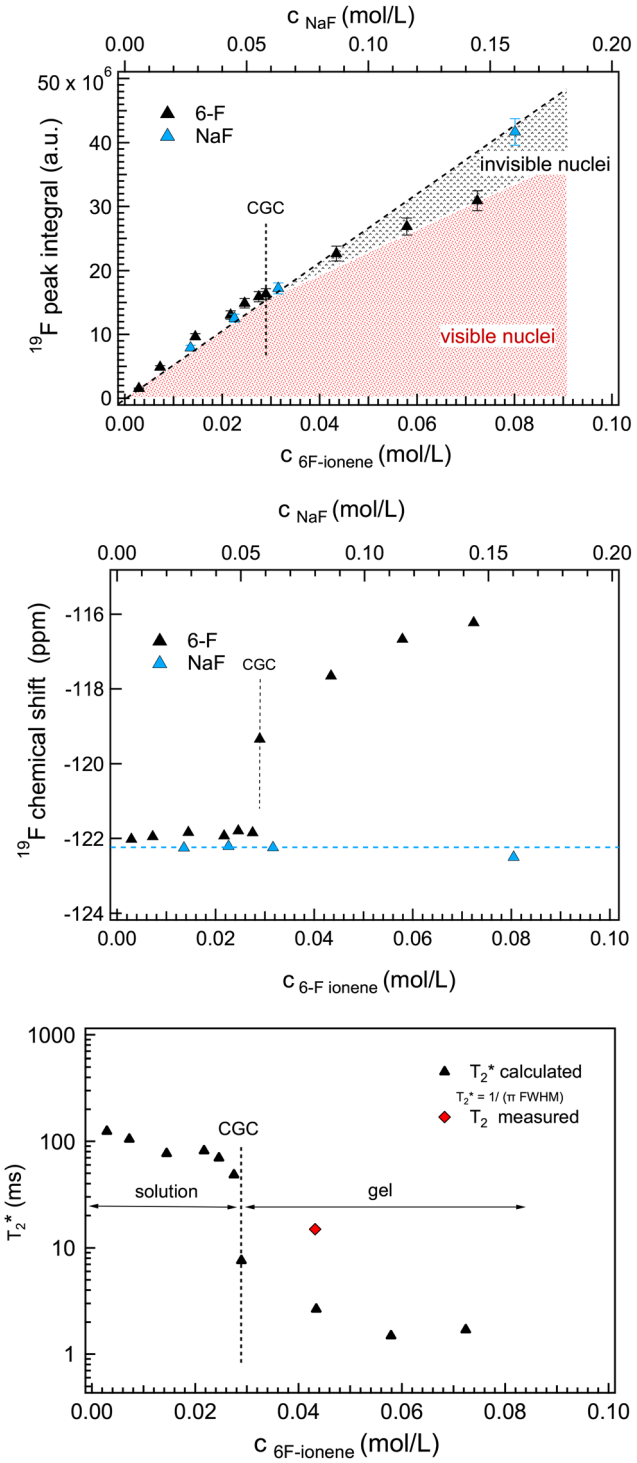

Fig. 7 (top) Integrated intensities of NMR peaks for ^{19}F nuclei as a function of 6-F concentration in D_2O. CGC is marked by a black dashed vertical line. (center) Position of the singlet obtained in ^{19}F NMR spectra of the ionene series and a reference NaF series, for which a narrow sharp singlet is observed at all concentrations. Error bars are smaller than the symbol size. (bottom) T_2^* relaxation time as a function of 6-F concentration, calculated from FWHM of the ^{19}F singlet. The red diamond marker presents the "true" T_2 value obtained using Carr–Purcell sequence with Gill–Meiboom modification. Error bars represented by the symbol size.

nuclei in the 6-F solutions are indeed visible, as was assumed already for the case of the H_b protons in Fig. 4. The loss of a subfamily of fluoride counterions to solution NMR in the gel region confirms previous observations of counterions being involved in the chain–chain crosslinking in ionene-based gels. Our study combining small-angle neutron and X-ray scattering (SANS and SAXS) has indeed given evidence to counterions being part of the cross-linking nodes. More precisely, SAXS shows counterion-counterion correlation peaks at distances corresponding to the inter-chain cross-links, suggesting that the cross-links are "rich" in F^- ions.[12,13] The literature suggests that apart from π–π stacking of the aromatic moieties, chain–chain crosslinks in ionene-based gels involve also cation–π, anion–π interactions, as well as indirect hydrogen bonding *via* anions and the solvent.[10,42,43] This is further corroborated by comparing in detail the chemical shifts and relaxation times of ^{19}F nuclei in the 6-F solution and gel phase, as discussed below.

Fig. 7 (center) compares the chemical shifts of the NaF reference system and 6-F solutions/gels. Fig. 7 (bottom) presents the apparent transverse relaxation time T_2^*, calculated from the full width half maximum (FWHM) of the fluoride peak according to $T_2^* = \frac{1}{\pi \mathrm{FWHM}}$. Firstly, fluoride peak in 6-F solutions has indeed an almost identical shift to the NaF reference (a sharp singlet is observed in both). Upon gelation, the environment experienced by ^{19}F nuclei changes drastically: at CGC, all fluoride counterions are still visible, but a downfield shift of 3 ppm is seen, together with a significant peak broadening, represented by a drop of the T_2^* by approximately one order of magnitude. This attests to the drastic increase in local interactions of the fluoride ions. Beyond CGC, an increasing proportion of fluoride ions becomes simply invisible, while the rest undergoes a further downfield shift and decreased T_2^* relaxation time. Other studies reported similar behaviour in a physical hydrogel formed by the self-assembly of a fluorine-containing dipeptide.[44] A weak deshielding effect on fluorine signals was observed, due to the formation of halogen–hydrogen bonds through the fluorine atoms in the dipeptide. In Fig. 6, we have also included a measurement of the "true" transverse relaxation time T_2 using the Carr–Purcell sequence for the gel sample at 24 g L^{-1} ($T_2 \sim 20$ ms). Due to magnetic field inhomogeneities, T_2^* is shorter than the "true" T_2. Thus, in the solution state, T_2 has to be at least 100 ms. Consequently, even if not measured for all concentrations, T_2 itself must experience a drop of at least one order of magnitude between the solution and gel states. The drop of relaxation time (or increased relaxation rate) of polyelectrolyte counterions in the presence of chain cross-linking has indeed been reported in the past, for example in studies of cross-linked polystyrene sulfonate, where the counterion was the quadrupolar ^{23}Na nucleus.[45] While the relaxation mechanisms of dipolar nuclei (^{19}F here) and quadrupolar nuclei are not the same, the presence of dynamic constraints of the polymer chains has the same qualitative effect on both types of nuclei.

^{19}F PFG-NMR was equally used to measure the average self-diffusion coefficients of fluoride counterions in the 6-F

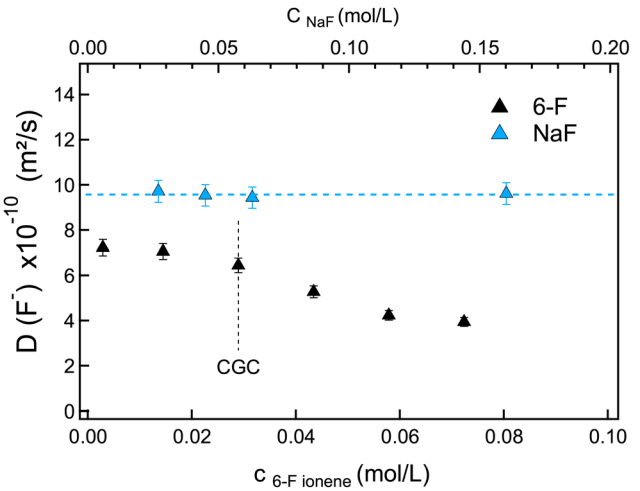

Fig. 8 Self-diffusion coefficient of fluoride ions in the NaF reference system and in 6-F solutions/gels. Measurements done at 18 °C.

solutions/gels and comparison was made to the NaF reference. In the case of fluoride ions in the gels and in the NaF reference, the decay of the signal in PFG-NMR was well described by a mono-exponential decay (see Fig. S6 of SI). The data are summarised in Fig. 8. The reference NaF system yields a constant value of the fluoride ion self-diffusion equal to $9.6 \pm 0.2 \times 10^{-10}$ m^2 s^{-1}. In 6-F solutions (all counterions are visible), the fluoride ion diffusion reaches approximately 70% of this reference value. At CGC (all counterions still visible), contrary to the sharp drop of T_2^*, no significant decrease in the fluoride diffusion coefficient is observed. At higher 6-F gel concentrations, the visible fluoride ions diffuse at 40% of the reference value, which is a similar percentage to that seen for the diffusion of visible chains in the gel phase (refer back to Fig. 5).

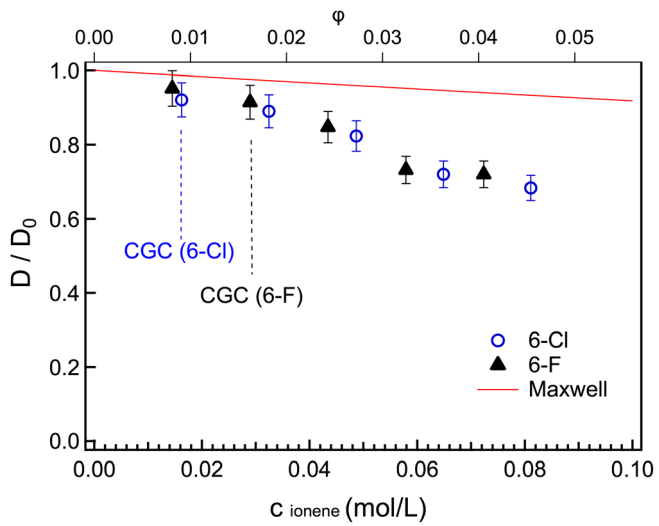

Fig. 9 Self-diffusion of water in 6-F and 6-Cl solutions and gels, normalised to the bulk self-diffusion coefficient of HDO contained in D_2O at 18 °C (1.64×10^{-9} m^2 s^{-1}). The secondary horizontal axis depicts the volume fraction (ϕ) occupied by ionene (at 0.1 mol L^{-1} this corresponds to 5.6%) and serves to plot the prediction of the simple Maxwell obstruction model, for which $D/D_0 = (1 - \phi)/(1 + \phi/2)$.[46]

3.3. Self-diffusion of water in ionene solutions and gels

In the case of water solvent protons, the decay of the signal in PFG-NMR was well described by a mono-exponential decay (see Fig. S7 of SI). Fig. 9 presents self-diffusion coefficients of the water solvent in 6-F and 6-Cl solutions and gels. It is presented as normalized to the bulk self-diffusion coefficient of HDO contained in D_2O at 18 °C (1.64×10^{-9} m^2 s^{-1}). The secondary horizontal axis depicts the volume fraction (ϕ) occupied by ionene (at 0.1 mol L^{-1} this corresponds to 5.6%) and serves to plot the prediction of the simple Maxwell obstruction model, for which $D/D_0 = (1 - \phi)/(1 + \phi/2)$.[46] This is considered as the upper bound and indeed our data fall beneath this prediction. No significant difference is observed for the 6-F and 6-Cl systems and no abrupt decrease is seen at the CGCs. In light of the literature on hydrogels, we do not consider the latter observation as surprising, water solvent molecules indeed retain much of their mobility on the transition from solution to gel.[31,35]

At the highest ionene concentration, the water self-diffusion coefficient falls to 70% of the bulk water value. In comparison to the ionene counterions (decrease to 40% of the NaF reference value for the visible fluoride ions), this decrease is less significant, attesting to the expected weaker interaction of water with the ionene chains than for the counterions, which take part in the chain–chain crosslinking. Weak interactions of water with ionene chains in ionene-based hydrogels was previously seen by NMR relaxation measurement of water protons.[47] Ionene hydrogels shows low proton relaxation rates between 0.33 s^{-1} and 0.4 s^{-1}, only slightly higher than the relaxation rate of protons in bulk water (0.3 s^{-1}), and with a very weak frequency dependence.

Conclusion

NMR (^{1}H and ^{19}F) was employed here to study the changes taking place in aqueous systems of 6-F and 6-Cl gel-forming ionenes, upon the transition from the solution/liquid to the gel state. ^{1}H NMR signal of ionene benzene protons was taken to probe the behaviour of the ionene chains, and, in the case of 6-F systems, ^{19}F NMR gave information on the chain counterions. For the ionene chains, the most visible signature of gelation is a significant loss of ^{1}H NMR peak intensity at CGC. This is the clearest in the case of 6-F ionene, where good solubility in water is guaranteed and all ionene chains are visible to ^{1}H NMR in the solution phase. We interpret the signal loss as the onset of chain–chain cross-linking (*e.g.* π–π stacking), which leads to a fast NMR relaxation of the benzene proton nuclei and thus loss of the ^{1}H NMR signal to liquid state NMR detection. The proportion of "invisible" ionene chains in the gel phase is significant, it increases with ionene concentration and reaches over 80% of the total signal at the highest gel concentrations considered. The chains remaining visible in the gel state retain

the same chemical shift. This is contrary to some observations where a visible downfield/upfield shift of aromatic protons was reported, as in gel-forming polyimide solutions,[48] while others report zero shift of aromatic protons and highlight a shift of amide protons (due to hydrogen bonding).[33]

For the counterion behaviour (probed only for the case of 6-F ionenes), gelation demonstrates itself at the CGC by (a) a sudden downfield shift of 3 ppm of the ^{19}F NMR peak and (b) a drop in the ^{19}F relaxation time (T_2^*, related to peak width) by more than one order of magnitude, but all this without any loss of peak intensity. Beyond CGC, further downfield shift is observed as well as slightly lower relaxation time and now a signal loss also appears (reaching only 25% at the highest gel concentration). It is clear that as chain–chain cross-linking takes place in ionene-based hydrogels, the mobility of the chains as well as counterions decreases, leading to faster relaxation and ultimately to signal loss for a given proportion of chains/counterions. However, the changes are not as abrupt for the counterions, as they are for the chains. We have indeed previous SAXS data strongly suggesting that ionene counterions are involved in the chain–chain cross-linking[13] and mechanism such as anion–π interactions and indirect hydrogen bonding *via* anions and the solvent have been suggested.[10,42,43]

If we place ourselves in the fast exchange hypothesis, exchange between "free" and "immobilized" chains/counterions being faster than the NMR time-scale, all presented NMR observables (chemical shifts, relaxation rates and diffusion coefficients) are a mole fraction weighted average of the two states.[49,50] For the case of the fluoride counterions, the NMR observable that seems to be particularly sensitive to the difference between the two states is the transverse relaxation rate (inverse of the T_2 relaxation time), which is consistent with literature.[51,52] To proceed further in applying the fast exchange model, we lack however information on the mole fractions for each of the states. At this stage it is not clear whether in order to interpret simultaneously the integral loss, the displacements of the chemical shifts and the relaxation rates, it is necessary to evoke a model with two states, or indeed three. NMR measurements based on saturation transfer difference would be most helpful to make visible the fraction of fluoride counterions (and chains) lost to solution state NMR.[35,51] Equally, it would be interesting to extend our observations to HOESY measurements, which indicate which pairs of nuclei are communicating in the NMR sense of the term (*i.e.* close in space), in particular for the couple ^{1}H-^{19}F.

Changes in diffusion coefficients for the visible ionene chains and counterions around the liquid-gel transition are not spectacular, in comparison to the loss of signal for the chains and the drop in relaxation times for counterions at the CGC mentioned above. In the gel phase, the visible chains and counterions diffuse with a diffusion coefficient lower than in the solution phase by a factor of 2 at most. One interesting observation is the systematically slower chain diffusion in the 6-F solutions and gels, as opposed to 6-Cl (a factor of 2). This is attributed to two reasons. First the more dissociated form of counterions in the case of F^- as opposed to all other halide ions observed by previous scattering and simulations studies of solutions of conventional ionenes.[17–19,41] This dissociation of F^- ions renders the chains more charged and thus more rigid, lowering their diffusion coefficient as is the case for solutions of conventional ionenes.[19] The second reason is linked to the presence of a tighter mesh size measured by SAXS for F-ionene gels, a phenomenon that is accentuated as the gel concentration increases.[13] A denser network of cross-links would indeed also lead to a decreased self-diffusion coefficient of the free non-crosslinked chains within such network. As the faster diffusion of 6-Cl chains is present across the entire concentration range, the first explanation evoking chain rigidity carries more weight. Finally, diffusion of water solvent in ionene gels decreases down to 70% of the bulk water value at the highest gel concentrations. This is below the upper bound predicted by the Maxwell model, but attests to relatively weak water–ionene interactions, as suggested by previous frequency-dependent NMR relaxation measurements.[47]

Overall, NMR measurements on ionene chains and counterions have allowed us to characterise the matrix dynamics in ionene-based gels and highlight the differences brought by the nature of the counterion, for which these gels are known for. The next step is to investigate how the matrix chain rigidity in ionene gels with different counterions could influence the diffusion of guest species (charged molecules or colloids), with a size both above and below the typical ionene gel mesh-size (around 20 nm).[12,13]

Author contributions

SM: investigation, resources, formal analysis, writing – original draft; LT: investigation, supervision, writing – review & editing; JSP: investigation, supervision, writing – review & editing; FR: investigation, formal analysis, supervision, writing – review & editing; NM: conceptualization, methodology, writing – review & editing, visualization, supervision, project administration, funding acquisition.

Conflicts of interest

There are no conflicts to declare.

Data availability

Data for this article, including the raw NMR spectra and the identity of all samples, are available on Zenodo at **https://doi.org/10.5281/zenodo.15690691**.

Supplementary information: additional NMR spectra of ionene precursor, 6-Cl ionene in DMSO/D_2 O, PFG-NMR signal decays. See DOI: **https://doi.org/10.1039/d5cp02615f**.

Acknowledgements

The authors acknowledge Delphine Talbot for thermogravimetric measurements and Guillaume Mériguet for helpful discussions on NMR.

References

1 *Polymer gels: fundamentals and applications*, ed. H. B. Bohidar, P. Dubin, Y. Osada and A. C. Society, American Chemical Society; Distributed by Oxford University Press, Washington, DC: [Cary, NC], 2003.
2 R. Netz and D. Andelman, *Phys. Rep.*, 2003, **380**, 1–95.
3 A. Y. Grosberg, T. T. Nguyen and B. I. Shklovskii, *Rev. Mod. Phys.*, 2002, **74**, 329–345.
4 C. Poinsignon, *Mater. Sci. Eng., B*, 1989, **3**, 31–37.
5 A. N. Zelikin, D. Putnam, P. Shastri, R. Langer and V. A. Izumrudov, *Bioconjugate Chem.*, 2002, **13**, 548–553.
6 W. Jaeger, J. Bohrisch and A. Laschewsky, *Prog. Polym. Sci.*, 2010, **35**, 511–577.
7 H. Kourai, T. Yabuhara, A. Shirai, T. Maeda and H. Nagamune, *Eur. J. Med. Chem.*, 2006, **41**, 437–444.
8 S. Punyani and H. Singh, *J. Appl. Polym. Sci.*, 2006, **102**, 1038–1044.
9 M. Hess, R. G. Jones, J. Kahovec, T. Kitayama, P. Kratochvíl, P. Kubisa, W. Mormann, R. F. T. Stepto, D. Tabak, J. Vohlídal and E. S. Wilks, *Pure Appl. Chem.*, 2006, **78**, 2067–2074.
10 Y. Misawa, N. Koumura, H. Matsumoto, N. Tamaoki and M. Yoshida, *Macromolecules*, 2008, **41**, 8841–8846.
11 J. Bachl, O. Bertran, J. Mayr, C. Alemán and D. Díaz Díaz, *Soft Matter*, 2017, **13**, 3031–3041.
12 C. Hotton, J. Sirieix-Plénet, G. Ducouret, T. Bizien, A. Chenneviere, L. Porcar, L. Michot and N. Malikova, *J. Colloid Interface Sci.*, 2021, **604**, 358–367.
13 C. Hotton, G. Ducouret, J. Sirieix-Plénet, T. Bizien, L. Porcar and N. Malikova, *Macromolecules*, 2023, **56**, 923–933.
14 C. Hotton, G. Ducouret, J. Sirieix-Plénet, T. Bizien, C. Guibert, P. Levitz, L. Michot and N. Malikova, *Appl. Clay Sci.*, 2024, **255**, 107392.
15 P. J. Moncure, Z. C. Simon, J. E. Millstone and J. E. Laaser, *J. Phys. Chem. B*, 2022, **126**, 4132–4142.
16 F. Arends, R. Baumgärtel and O. Lieleg, *Langmuir*, 2013, **29**, 15965–15973.
17 N. Malikova, S. Cebašek, V. Glenisson, D. Bhowmik, G. Carrot and V. Vlachy, *Phys. Chem. Chem. Phys.*, 2012, **14**, 12898–12904.
18 N. Malikova, A.-L. Rollet, S. Cebašek, M. Tomšic and V. Vlachy, *Phys. Chem. Chem. Phys.*, 2015, **17**, 5650–5658.
19 C. Hotton, Y. Sakhawoth, A.-L. Rollet, J. Sirieix-Plénet, L. Tea, S. Combet, M. Sharp, I. Hoffmann, F. Nallet and N. Malikova, *C. R. Chim*, 2024, **27**, 1–13.
20 S. Marbach, D. S. Dean and L. Bocquet, *Nat. Phys.*, 2018, **14**, 1108–1113.
21 J. Bezençon, M. B. Wittwer, B. Cutting, M. Smieško, B. Wagner, M. Kansy and B. Ernst, *J. Pharm. Biomed. Anal.*, 2014, **93**, 147–155.
22 K. Hatada and T. Kitayama, *NMR Spectroscopy of Polymers*, Springer Berlin Heidelberg, Berlin, Heidelberg, 2004, pp. 169–197.
23 B. Šarac, G. Mériguet, B. Ancian and M. Bešter-Rogac, *Langmuir*, 2013, **29**, 4460–4469.
24 M. Giesecke, G. Mériguet, F. Hallberg, Y. Fang, P. Stilbs and I. Furó, *Phys. Chem. Chem. Phys.*, 2015, **17**, 3402–3408.
25 G. Hostnik, M. Boncina, C. Dolce, G. Meriguet, A.-L. Rollet and J. Cerar, *Phys. Chem. Chem. Phys.*, 2016, **18**, 25036–25047.
26 H. Walderhaug, O. Söderman and D. Topgaard, *Prog. Nucl. Magn. Reson. Spectrosc.*, 2010, **56**, 406–425.
27 M. G. Oostwal, M. H. Blees, J. De Bleijser and J. C. Leyte, *Macromolecules*, 1993, **26**, 7300–7308.
28 T. Nose, *Annual Reports on NMR Spectroscopy*, Elsevier, 1993, vol. 27, pp. 217–253.
29 H. Yasunaga and I. Ando, *Polym. Gels Networks*, 1993, **1**, 83–92.
30 J. E. Tanner, *J. Chem. Phys.*, 1970, **52**, 2523–2526.
31 D. Woessner and B. Snowden, *J. Colloid Interface Sci.*, 1970, **34**, 290–299.
32 C. Johnson, *Prog. Nucl. Magn. Reson. Spectrosc.*, 1999, **34**, 203–256.
33 T. Shao, M. Noroozifar and H.-B. Kraatz, *Soft Matter*, 2024, **20**, 2720–2729.
34 Y. E. Shapiro, *Prog. Polym. Sci.*, 2011, **36**, 1184–1253.
35 P. Li, C. Malveau, X. X. Zhu and J. D. Wuest, *Langmuir*, 2022, **38**, 5111–5118.
36 B. Nystrom, H. Walderhaug and F. K. Hansen, *J. Phys. Chem.*, 1993, **97**, 7743–7752.
37 S. G. Baldursdóttir, A.-L. Kjøniksen and B. Nyström, *Eur. Polym. J.*, 2006, **42**, 3050–3058.
38 K. Persson, P. Griffiths and P. Stilbs, *Polymer*, 1996, **37**, 253–261.
39 B. Rao, Y. Uemura, L. Dyke and P. M. Macdonald, *Macromolecules*, 1995, **28**, 531–538.
40 K. Thuresson, S. Nilsson, A.-L. Kjøniksen, H. Walderhaug, B. Lindman and B. Nyström, *J. Phys. Chem. B*, 1999, **103**, 1425–1436.
41 M. Druchok, V. Vlachy and K. A. Dill, *J. Chem. Phys.*, 2009, **130**, 14270–14276.
42 J. Bachl, D. Zanuy, D. E. López-Pérez, G. Revilla-López, C. Cativiela, C. Alemán and D. D. Díaz, *Adv. Funct. Mater.*, 2014, **24**, 4870.
43 S. K. Kundu, T. Matsunaga, M. Yoshida and M. Shibayama, *J. Phys. Chem. B*, 2008, **112**, 11537–11541.
44 P. Ravarino, D. Giuri, D. Faccio and C. Tomasini, *Gels*, 2021, **7**, 43.
45 R. Tromp, J. Van Der Maarel, J. De Bleijser and J. Leyte, *Biophys. Chem.*, 1991, **41**, 81–100.
46 E. L. Cussler, *Diffusion: mass transfer in fluid systems*, Cambridge University Press, 1st edn, 2009.
47 C. Hotton, PhD thesis, Sorbonne Université, Paris, France, 2022.
48 J. Wen, S. Jiang, J. Wang, X. Li, Z. Bi, Y. Jin, L. Fan, L. Wang, Y. Wu and F. Gan, *Polymer*, 2023, **278**, 126006.
49 L. Fielding, *Tetrahedron*, 2000, **56**, 6151–6170.
50 T. D. W. Claridge, *High Resolution NMR Techniques in Organic Chemistry*, Elsevier, 2009.
51 R. Novoa-Carballal, M. Martin-Pastor and E. Fernandez-Megia, *ACS Macro Lett.*, 2021, **10**, 1474–1479.
52 D. E. Demco and A. Pich, *Macromol. Chem. Phys.*, 2023, **224**, 2200410.

